Primljen / Received: 27.5.2022.
Ispravljen / Corrected: 21.11.2022.
Prihvaćen / Accepted: 29.12.2022.
Dostupno online / Available online: 10.2.2023.

Effect of glass sand used as aggregate on micro-concrete properties

Author:

Assist.Prof. **Serkan Etli**, PhD. CE
Munzur University, Tunceli, Turkey
Department of Emergency Aid and Disaster Management
serkanetli@munzur.edu.tr
Corresponding author

Research Paper

Serkan Etli

Effect of glass sand used as aggregate on micro-concrete properties

Micro-concrete (MC) can be defined as a high-performance cement-based material produced using microaggregates and cement in the required proportions. Owing to its high performance, it has the potential to be used in the structural repairs of existing building elements. Within the scope of this study, an evaluation was conducted by creating a usage scenario under which glass, which is a waste product, can be reduced and applied in a way that provides a sufficient MC performance. There are four different binder contents in the mixtures within the scope of the present study, i.e., 570, 580, 599, and 658 kg/m^3. From these mixtures, together with the control mixture, 12 %, 27 %, and 50 % microaggregates were replaced with glass sand and 16 different mixtures with a total of 4 different aggregate contents were produced. For the mechanical, physical, and durability tests, 40 × 40 × 160 mm sized prisms and 50 × 50 × 50 mm sized cubes were produced. For the purposes of this research, mechanical tests were carried out on 144 7-, 28- and 56-day old prismatic specimens. In addition, the effects of a freeze-thaw and temperature on the mechanical properties were investigated on 192 prismatic samples. In determination of the durability, physical properties such as the porosity, sorptivity, and specific gravity were tested and determined using cubic samples. The test results show that the replacement of MA with GS has positive effects on all mechanical behaviours of MC.

Key words:
glass sand, micro-conrete, freezing/thawing, mechanical properties

Prethodno priopćenje

Serkan Etli

Učinak recikliranog stakla kao agregata na svojstva mikrobetona

Mikrobeton je visoko učinkovit materijal na bazi cementa koji se proizvodi upotrebom mikrogregata i cementa u točno određenim omjerima. Zbog iznimno visokih performanci, taj materijal ima potencijal za korištenje kod konstrukcijskih popravaka postojećih građevinskih elemenata. U sklopu ovog rada provedena je evaluacija izradom scenarija uporabe prema kojem se staklo, koje je otpadni proizvod, može usitniti i primijeniti na način koji osigurava dovoljnu izvedbu mikrobetona. Postoje četiri različita udjela veziva u smjesama u okviru ovog istraživanja, tj. 570, 580, 599 i 658 kg/m^3. U spomenutim je smjesama, kao i u kontrolnoj smjesi redom 12 %, 27 % i 50 % mikroagregata zamijenjeno recikliranim staklom, te je na taj način proizvedeno ukupno 16 različitih mješavina sa četiri različita udjela agregata. Za mehanička i fizikalna ispitivanja te ispitivanja svojstva trajnosti proizvedene su kocke veličine 50 × 50 × 50 mm i prizme veličine 40 × 40 × 160 mm. Za potrebe ovog istraživanja provedena su mehanička ispitivanja na 144 uzorka starosti 7, 28 i 56 dana. Osim toga, na 192 uzorka prizme ispitan je utjecaj smrzavanja i odmrzavanja i općenito učinka temperature na mehanička svojstva. U određivanju svojstva trajnosti ispitivana su fizikalna svojstva kao što su poroznost, sorptivnost i specifična gustoća, a određivana su testovima na uzorcima u obliku kocke. Rezultati ispitivanja pokazuju da zamjena mikroagregata s recikliranim staklom ima pozitivne učinke na sva mehanička ponašanja mikrobetona.

Ključne riječi:
reciklirano staklo, mikrobeton, smrzavanje/odmrzavanje, mehanička svojstva

1. Introduction

The aim of this research is to contribute toward the protection of the natural environment by absorbing the waste in micro-concrete (MC). A large amount of cement is used to improve the mechanical properties and utilisation of cement-based materials. Portland cement, the energy use of which is intense during production, accounts for approximately 5 % of global anthropogenic carbon dioxide emissions. Pozzolanic additives consisting of waste glass derivatives, which are randomly stored or placed in landfills, make a significant contribution to the sustainability of concrete production and thereby the cement industry. In addition, the glass waste produced, which has an amorphous structure and is non-biodegradable, as a harmful effect on natural environments. Glass bottles and containers used for the storage and protection of food and beverages are also left to nature as domestic waste after such products are consumed, taking glass waste a ubiquitous by-product. In addition, fine glass dust, even in soil, seriously harms living organisms. More importantly, the qualities of glass powder, if ground to a certain degree, create a new understanding of its intended use.

The development of high-performance materials such as self-compacting concrete and reactive powder concrete have elicited the attention of researchers. Considering the effectiveness of superplasticizers, which are frequently used in the development of cement-based building materials, another production parameter, microaggregates (MA), has been intensively studied. Self-compacting concrete and reactive powder concrete require the use of fine materials supplied in large quantities directly from nature or soil through processing. Owing to the use of superplasticizers, mixtures can be added to a fresh mixture without segregation, the grain packing density can be improved, and the workability can be increased. Increasing the workability also helps in creating the desired rheological properties. With such material, a noticeable increase in the mechanical properties can be observed by reducing the water–cement value, which represents the basic strength parameter. This also increases the durability of the concrete derivative by improving the distribution of the micropores and nanopores formed in the matrix. In this way, it can be applied with concrete having finer micro-materials (concrete with producible application materials) [1–4]. Concrete with a thinner material (micro concrete) can also be produced, applications can be made at the desired depth during repair and during a surface application, and micro-cracks can be easily repaired.

Some of the above-mentioned fine or regular powders obtained as a natural or processed material are unprocessed or industrially produced by-products. Industrial waste by-products can cause problems, including an expensive or impossible recycling process. It is also important to reduce emissions released into the atmosphere during cement production, which are dangerous for human health and the environment. To do so, it is important to use binder materials that can be disposed of as waste instead of cement. In addition to saving energy during the production process, such materials can be easily recycled, decreasing the amount of environmental pollution by saving raw materials and reducing the effects of environmental pollution [5–8]. Glass powder has been successfully used as a mineral additive in place of cement (up to 30 %) [8–12]. Aliabdo et al. [13] stated that the use of 10 % glass powder instead of cement increases the compressive strength of mortar by approximately 9 %. Similar study results were obtained by Grdić et al. [14], who demonstrated almost a 6.5 % increase in compressive strength using a glass substitution.

In addition, when considering high-performance concrete designs, it should be noted that semi-inert MA including finely ground limestone or quartz can be used. This activity has been consistently observed in studies on the rheological properties of high-strength concrete applying MA. More importantly, a concrete matrix, owing to its tendency to increase the amount of MA in a system, can help reduce or eliminate the use of coarse aggregates and sand if its feasibility and engineering suitability are proven [2, 15].

It has been determined that the use of various natural pozzolanic materials in cement and urban structures may gradually increase, along with durable waste containing siliceous and aluminous substances produced as commercial by-products. Owing to their strength, it is understood that such materials provide significant improvements in the mechanical properties of concrete mixtures [16]. Industrial waste such as blast furnace slag, fly ash, silica fume, and slag have been used as raw materials and components in the cement industry for many years. Agricultural residues such as rice husk ash in the production of concrete and cement is a striking example of such use. However, there are many types of industrial waste, including glass products, that have yet to be used in this sector or that do not contain sufficient data despite their application. In fact, successful studies on the potential uses of finely ground waste glass have been conducted, and an enhancement in the strength of concrete derivatives when this material is used as an alkali-silica reactivity-based pozzolanic material has been observed [17, 18]. Examining its manufacturing procedure, such glass is shaped using aggregates of multiple raw inorganic minerals that become a hard, homogeneous, stable, inert, amorphous, and isotropic fabric after a managed cooling procedure. Looking at its significant composition, glass can be divided into many different categories. In addition, soda-lime glass is normally used in the manufacturing of tin and flat glass. As a result of this type of manufacturing, more than 80 % of waste glass is formed at the end-of-life stage based on weight [17]. Such glass can be used for damage (macro- or micro-cracks occurring in concrete shells and spills) that occurs in the structural elements of reinforced concrete systems at a certain stage of their service life. Owing to the material use and production of MC, such damage can be easily repaired [19]. In addition, owing to its high binding feature, it can also be used for the sewing reinforcement anchors during reinforcement operations [20].

The main purpose of this study is to investigate the changes in the mechanical and durability properties of MC, which contains

Table 1. Chemical composition of Portland cement and tile dust

Chemical composition [%]	Portland cement	Silica fume	Glass sand (0.063–0.125 mm)	Limestone powder (0–1 mm)
SiO_2	19.79	90.75	70.85	0.56
AlO_3	3.96	-----	-----	-----
Al_2O_3	3.85	0.72	0.85	0..16
Fe_2O_3	4.15	2.29	0.23	0.14
CaO	61.84	0.56	8.84	57.9
MgO	3.22	-----	-----	0.7
K_2O	-----	1.51	0.24	-----
Na_2O	-----	0.55	14.41	-----
SO_3	2.32	0.51	0.23	-----
P_2O_5	-----	-----	0.55	-----
TiO	-----	-----	-----	-----
Cr_2O_3	-----	-----	-----	-----
Mn_2O_3	-----	-----	-----	-----
MgO	-----	-----	3.8	-----
Loss of ignition	0.87	3.11	-----	-----
Blaine [m^2/kg]	326	21080	-----	-----

four different GS substitutes and four different binder dosages. In addition, the effects of temperature on the mechanical properties of the samples were also evaluated for the produced binders and the substituted GS. A total of 16 mixtures produced were subjected to testing. After grinding the waste glass products, a 0.063–0.125 mm material sieve gap was used. Sand obtained by crushing limestone-based rocks was used as MA. By contrast, MA produced within a sieve range of 0–4 mm was used by sieving this sand through a 1-mm sieve. Axial compression and flexural tensile strength tests were conducted on the samples produced on the 7th, 28th, and 56th days. In addition, the freeze-thaw effect (between -18 °C and +5 °C) and the absorbency properties were tested in terms of the durability. The porosity and specific gravity were investigated for changes in the physical properties.

2. Materials and experimental campaign

The methodological procedure regarding the materials used in this study and the proportions of the mixtures produced are included in the sub-headings. A brief flowchart of the study methodology is given in Figure 1. The mixtures were produced in four groups. Silica fume (SF) was used at 18 % of the total binder content in each batch of mixture. The SF content chosen was within the ratios obtained from other studies in the literature [2, 21, 22]. Binder (cement + silica fume) dosages of 570, 580, 599, and 658 kg/m^3 were used in each mixture group. In the mixtures produced, 0 %, 12 %, 27 %, and 50 % GS (0.063–0.125 mm) by weight was used instead of MA (0–1 mm). As a result, a total of 16 mixtures were produced within the scope of the study. In the group of mixtures produced, 40 × 40 × 160 mm^3 sized prism samples were produced for the mechanical testing of each mixture. In addition, three cube-shaped samples with dimensions of 50 × 50 × 50 mm^3 were produced from each mixture for the absorbency tests. The mechanical properties, temperature curing effect, freeze-thaw, sorptivity, and physical properties were investigated. A total of 336 prism-shaped samples and 48 cube-shaped samples were used in the experiments.

Figure 1. Experimental workflow

2.1. Materials

Silica fume and CEM-I 42.5R Portland cement were used as binders in the mixtures produced within the scope of the present study. Crushed sand obtained from limestone in the mixtures was sieved through a 1-mm perforated sieve and separated into MA. The chemical properties of silica fume, MA (limestone dust), and cement are given in Table 1. In addition, glass bottles that accumulate as domestic waste in nature, particularly bottles where liquid substances are stored (such as soda/mineral water) were collected and were ground into glass sand (GS). The resulting powder was sieved and used as MA. Sieve analyses of the MA obtained by sieving and the GS obtained from recycling are given in Figure 2.

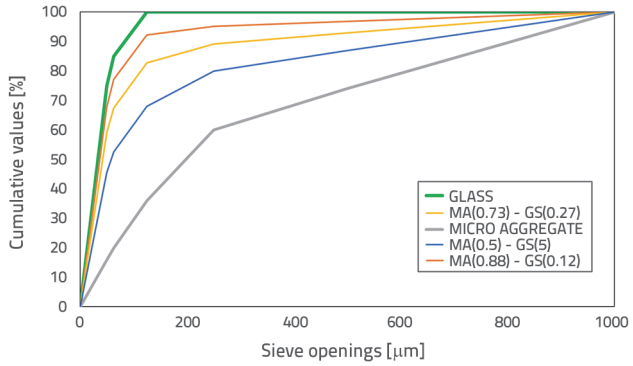

Figure 2. Sieve analysis of materials

In addition, water and a superplasticizer, namely a polycarboxylate ether-based water reducing chemical additive (HRWRA), were used to increase the workability of the mixtures. In this way, the aim is to maintain the homogeneity of the produced mixtures as well as achieve high fluidity capacities. Cement, silica fume, MA, GS (Figure 3), and HRWR were used in the mixtures produced as MC. The specific gravity values of the cement, silica fume, MA, GS, and HRWR are 3.1, 2.2, 2.65, 2.56, and 1.055 t/m^3, respectively.

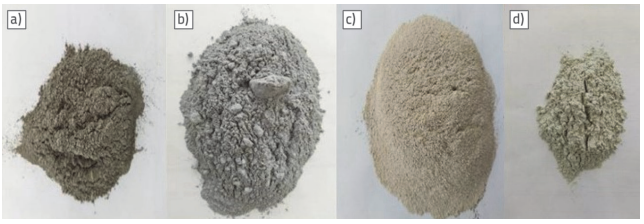

Figure 3. Mixture materials: a) cement, b) silica fume, c) MA, and d) GS

2.2. Mixture design

The MCs produced were homogeneously produced with the aid of a standard mortar mixer meeting the requirements of the current standard [23] until the total homogeneity of the mixture was observed during the preparation of the components. As summarised in Table 2, the water/binder (w/b) ratio was at a constant value of 0.535 in the mixtures. Mixtures were basically produced in four groups, and among these groups, the binder dosage was changed along with the aggregate content. The mixtures can be divided into four groups: MC1–MC4, MC5–MC8, MC9–MC12, and MC13–MC16. The amount of water was calculated as 371.8, 378.2, 390.8, and 429.3 kg/m3 for MC1–MC4, MC5–MC8, MC9–MC12, and MC13–MC16, respectively.

Table 2. Mixture design

Mixture mark	Cement [kg/m^3]	Water [kg/m^3]	Silica fume [kg/m^3]	HRWR [kg/m^3]	Micro aggregate [kg/m^3]	Glass sand [kg/m^3]
MC1	570	371.8	125	12	996.7	0
MC2	570	371.8	125	12	877.1	119.6
MC3	570	371.8	125	12	727.6	269.1
MC4	570	371.8	125	14	498.3	498.4
MC5	580	378.2	127	13	966	0
MC6	580	378.2	127	13	850.1	115.9
MC7	580	378.2	127	13	705.2	260.8
MC8	580	378.2	127	14	483	483
MC9	599	390.8	131.5	14	908.8	0
MC10	599	390.8	131.5	14	799.7	109.1
MC11	599	390.8	131.5	14	663.4	245.4
MC12	599	390.8	131.5	14	454.4	454.4
MC13	658	429.3	144.5	15	738	0
MC14	658	429.3	144.5	15	649.4	88.6
MC15	658	429.3	144.5	15	538.7	199.3
MC16	658	429.3	144.5	15	369	369

The chosen binder contents in the mixtures were 695, 707, 730.5, and 802.5 kg/m^3 for the same group arrangement, respectively. In addition, the amount of MA in the mixtures varies at 996.7, 966, 908.8, and 738 kg/m^3 for MC1–MC4, MC5–MC8, MC9–MC12, and MC13–MC16, and the rate of change between MA and GS used was 0 %, 12 %, 27 %, and 50 % by weight of the mixtures in each produced group (Table 2), respectively.

2.3. Sample facture and mixing procedure

The standard mixer shown in Figure 4a was used to produce the micro-concrete. During the production of the mixtures, the first dry mixture was made, and the mixer was operated for 1 min. Then, 2/3 of the required water amount was added to the mixture, which was mixed for 1 min. The required HRWR was added to the remaining 1/3 of the water and then added to the mixture and mixed for another 1 min. The mixture was then allowed to rest for 1 min and stirred for an additional 1 min. Finally, the mixtures, whose fresh property tests were completed, were placed in the moulds. A total of 5 min was required to produce the mixture. In addition, the flowability of the produced mixtures was checked, and the workability was measured using a mini-slump flow test. Images obtained during the mini-slump flow test are given in Figure 4b. The mini-slump flow test apparatus was manufactured as a truncated cone with a height of 60 mm and upper and lower diameters of 70 and 100 mm, respectively. The results of the mini-slump flow test increased with an increase in the GS substitution rate within the 190–240 mm diameter range. These values are close to those of the self-compacting cement paste results described in the literature [24]. The mixtures produced were filled into metal prism-shaped moulds with dimensions of 40 × 40 × 160 mm and cubic-shaped moulds of 50 × 50 × 50 mm in size (Figure 4c). The samples were removed from the moulds after 24 h (Figure 4d) and placed in curing tanks to cure with water at 20±2 °C (Figure 4e). The samples were cured at two different ages. Samples with a curing age of 7 days, representing an early age, and 28 days, indicating a normal age, were experimentally tested. For the first batch of testing, only 7-day cured samples were removed from the curing tank and tested. All remaining samples were removed when the normal curing time reached 28 days. Age tests of 28 and 56 days were conducted on these samples.

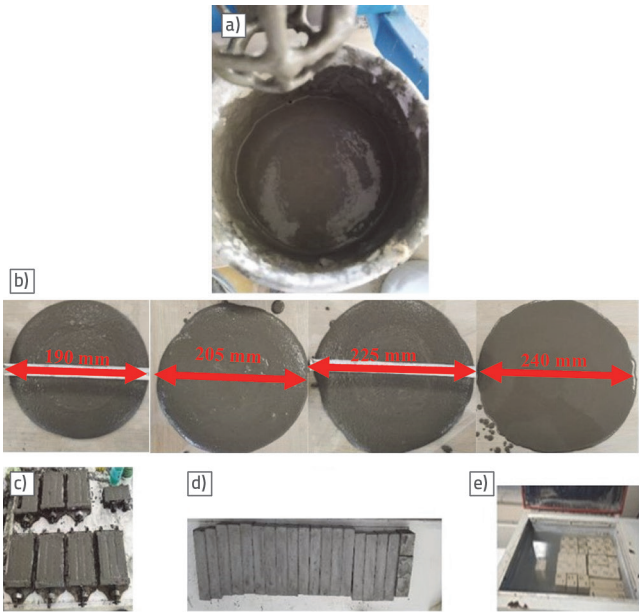

Figure 4. a) Mixer, b) slump flow c) moulding, d) demoulding, and e) water curing

2.4. Hardened state testing procedure

2.4.1. Mechanical testing procedure

The mixtures produced were removed from the moulds one day after being filled into metal moulds and cured in water saturated with lime at 20±2 °C. Within the scope of the present study, 7-, 28- and 56-day old samples were subjected to mechanical tests. For experimental studies at 7 and 28 days of age, samples taken from curing tanks at the relevant ages were taken to the laboratory environment and subjected to experiments. The remaining samples for the 56-day test were removed from the curing tank at the end of the 28-day curing period and stored in a laboratory environment until reaching 56 days. Three prisms were randomly selected from each design set for the test ages and subjected to a flexural strength test according to ASTM C348 [25]. An axial compressive strength test was conducted on parts consisting of broken prisms according to ASTM C349 [26] (Figure 5b). Test views of the hardened prisms are shown in Figure 5a.

Figure 5. a) Prisms for flexural strength and b) broken prisms after testing

2.4.2. Temperature cure effect

For the samples examined in the second group, the effect of temperature on the samples that completed the 28-day curing period was experimentally investigated. Nine prismatic samples were taken from each mixture in the curing tank, placed in a furnace, and exposed to heat, as shown in Figure 6. Temperature levels of 150 °C, 160 °C, and 180 °C were chosen for the thermal effects. During the experiment, all samples were placed in the furnace at the same time. To evaluate the temperature effect, the samples were removed from the furnace in three stages. The first batch of samples were tested by removing them from the oven 24 h after the oven had reached 150 °C. The second set of samples was tested 24 h after the oven temperature reached 160 °C. The last batch was removed and tested 24 h after the oven temperature had reached 180 °C (Figure 6). Three samples extracted for each temperature group effect were subjected to flexural tensile and compressive strength tests, and their averages were calculated.

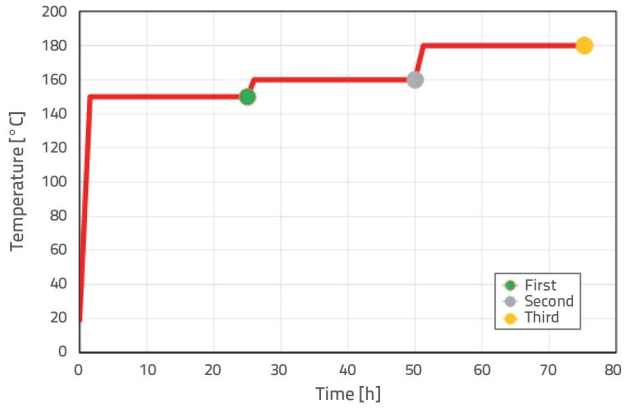

Figure 6. Temperature change

2.4.3. Freezing-thawing effect

The changes in strength of the MC mixtures produced under the influence of the freeze-thaw cycle were investigated. For this purpose, a freeze-thaw device with the cycle capacity to freeze in air and thaw in water was used. Within the scope of the study, the ASTM C666-97 "Standard Test Method For Resistance of Concrete to Rapid Freezing and Thawing" [27] was used for the freeze-thawing test of the MC samples. The test procedure requires that the concrete samples be subjected to the rapid freezing and thawing method in either water (Procedure A) or air (Procedure B). Within the scope of this test, the temperature during the freezing phase varies between 4 °C and −18 °C. It varies between −18 °C and 4 °C during the thawing phase. These cycles, consisting of freezing and thawing stages, take place between a period of 2–5 h (Figure 7). After the samples completed the 28-day water curing, three prism samples were taken from each mixture and placed in the device. After 100 cycles, the samples were removed from the instrument. For each mixture group, three prism samples were subjected to a test of their bending tensile strength, and the broken prism piece formed was then subjected to a compressive strength test of the samples.

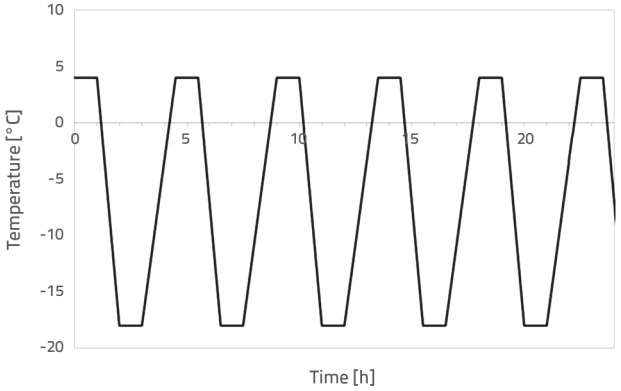

Figure 7. Frozen-thaw cycles

2.4.4. Sorptivity

A sorptivity test is used to measure the capillary water absorption for mortar or concrete. In other words, it is the measurement of the passage of water through the capillary structures formed between the internal structure and the surface in dry concrete or its derivatives. The measurement of this water transfer, also known as water absorption, is achieved by measuring the changes over time and plotting them on a graph. In products such as mortar, this test is typically conducted on cube-shaped samples. As a result, the measurements of the time-dependent changes in water absorbed from the element surfaces by the capillary structures formed by the combination of macro- and micro-voids in materials such as concrete or mortar can be defined as a sorptivity test [28, 29]. The absorbance test was carried out according to ASTM C1585-13 [30], and the cubic samples produced were removed from the curing tank after 28 days of water curing and subjected to this test. These samples taken from the curing tank were kept in an oven at 100±2 °C for 24 h until the sample weight remained constant. The main reason for this application is the evaporation of the existing water content in the sample followed by capillary water absorption. The samples were taken from the furnace and cooled at room temperature. Next, the four sides of the samples were coated with a waterproof material (e.g. paraffin). The upper and lower surfaces of the coated samples were left open. One of these two open surfaces is in contact with water, and the other surface is left in contact with air. The water absorption weights formed by the capillary system are then measured (Figure 8).

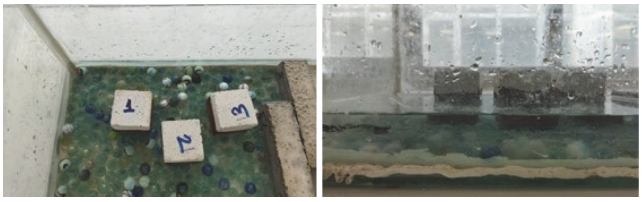

Figure 8. Sorptivity test set-up

After the sample met was placed in water, it was removed from the tank at the 5th, 10th, 30th, 60th, 240th, and 1440th minutes and weighed with an accuracy of 0.01 g. The relationship between the water absorption Q (m^3) and the square root of the measurement time is usually obtained as a graph, showing an almost linear variation. The capillary absorption coefficient (k) is given in Eq. (1) [30, 31]:

$$k = \frac{Q}{A \times \sqrt{t}} \quad (1)$$

To determine the sorption coefficient, the mass of water absorbed on the surface according to the change in the determined water absorption times are plotted on the graph. With the help of this diagram, sorption coefficients were determined using the values given in Eq. (2).

$$\frac{W}{A \times \rho} = S \cdot \sqrt{t} + I_0 \quad (2)$$

Here, W, A, and t are given as an increase in mass (kg), the area checked (m^2), and the time variable (min). By contrast, the S is the sorption coefficient at an early age ($mm/min^{1/2}$), and the value t is between 1 min and 7 h. The later age sorption coefficient is used when the t-value is more than 1 day. In Eq. (2), I_0 is defined as the initial sorption (mm), and is the water density (kg/m^3) [31].

2.4.5. Porosity, specific gravity, and bulk density tests

In previous studies, the porosity and density were shown to be effective in the evaluation of properties including the cohesion, discontinuity, and porosity of elements produced with concrete-derived materials [32, 33]. For MCs produced into 16 mixtures, the porosity, density, and specific gravity were calculated through experimental methods applied according to ASTM C-642 [34] on three cubes produced for each mixture. To calculate the porosity, density, and specific gravity values, the weights of the cube-shaped samples produced for all mixtures in saturated water were first measured, followed by the dry weights of the saturated surface. It was then left to dry in an oven at 100±2 °C for 24 h, and this drying process was continued until the weights stabilised. Experimental measurements using the mentioned standard have been conducted by researchers in other studies [35]. The following equations were used to calculate the porosity (Eq. (3)), specific gravity (Eq. (4)), and bulk density (Eq. (5)) of the samples according to ASTM C-642 [34].

$$\text{Porosity [\%]} = \frac{w_3 - w_1}{w_3 - w_2} \quad (3)$$

$$\text{Specific gracity} = \frac{w_1}{w_3 - w_2} \quad (4)$$

$$\text{Bulk density} = \frac{w_1}{w_1 - w_2} \quad (5)$$

Here, w_1 is the final weight of an oven-dried sample in air, w_2 is the measured weight of a fully saturated sample, and w_3 is the weight of a surface-dried saturated sample (Eqs. (3)–(5)).

3. Results and discussion

3.1. Flexural strength test results

3.1.1. Flexural strength for standard age

Within the scope of this study, the samples produced with micro-concrete were evaluated in three groups. The main reason for this is to test the usability of the samples produced by evaluating the impact of the environmental influences on the samples. In the first group, 7-, 28- and 56-day old samples were tested for their flexural tensile strength and evaluated mechanically depending on age. For the second group, 28-day samples were exposed to temperatures between 150 °C and 180 °C and then tested for their flexural tensile strength. For the third group, the flexural tensile strength after freeze-thaw effects was tested, and the changes in strength were compared with those of the 28-day samples.

The flexural tensile strength results under laboratory conditions for the first group of samples are examined within the scope of this section. To do so, tests were carried out on three samples produced for each mixture at ages of 7, 28, and 56 days. The results from these samples are presented in Figure 9 as the mean of all three samples for all MC mixes.

The MC13 mixture had the lowest flexural tensile strength among the 7-, 28-, and 56-day tests. The flexural tensile strength values obtained for the MC13 mixture for the 7-, 28- and 56-day experiments were calculated as 1.41, 2.88, and 3.01 MPa, respectively. In this mixture, the MA content is the lowest at 726 kg/m^3, and the binder content is the highest at 803 kg/m^3. As the result of the tests conducted at 7, 28, and 56 days of age indicate, among the mixtures produced, the maximum flexural tensile strengths of the samples produced from the MC4 mixture were reached. As the results of the experiments conducted on the MC4 mixture at 7, 28, and 56 days show, the flexural tensile strengths at these ages were found to be 1.97, 4.34, and 4.58 MPa, respectively. The MC4 mixture has the highest MA content of 985 kg/m^3 and contains 50 % GS. In addition, this mixture has the lowest binder content of 701 kg/m^3 (Figure 9).

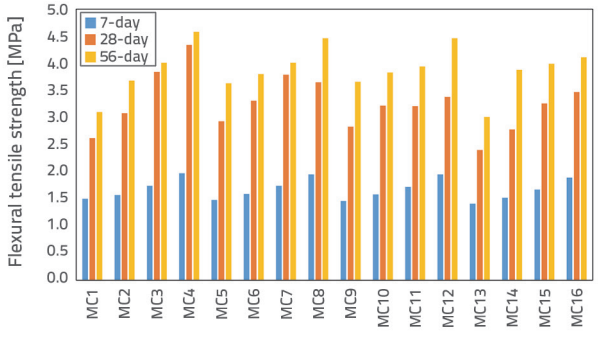

Figure 9. Flexural strength test results

A total of 16 mixtures were produced using four different GS and MA substitution ratios and four different binder contents. The groups produced were labelled as MC1–MC4, MC5–MC8, MC9–MC12, and MC13–MC16 mixtures, respectively, and MC1, MC5, MC9, and MC13 mixtures were designed as the control mixtures within each respective group. Within the scope of this section, samples produced from all mixtures were evaluated in terms of the tensile strength. Despite the increased binder content in the 7-day experiments, the control mixtures showed 1.3 %, 2.7 %, and 6 % reductions in the MC5, MC9, and MC13 mixtures, respectively, compared to MC1. In the 28-day experiments, the MC5 and MC9 mixtures showed an increase of 12 % and 8 %, respectively, compared to the MC1 mixture, whereas a decrease of 8.4 % was calculated for the MC13 mixture. In the 56-day experiments, the increase in the MC5 and MC9 mixtures reached 17 % and 18 %, respectively, compared to the MC1 mixture, whereas a 3 % decrease in the MC13 mixture was calculated (Figure 9). The GS-substituted mixtures among the MC1–MC4, MC5–MC8, MC9–MC12, and MC13–MC16 groups were compared with the control mixture in terms of their respective flexural tensile strengths obtained from the experiments. Increases of 16 % to 31 %, 18 % to 32 %, 18 % to 34 %, and 18 % to 34 % were calculated in the 7-day experiments, and increases of 47 % to 66 %, 25 % to 29 %, 13 % to 19 %, and 36 % to 45 % in the 28-day trials for the above groups, respectively. The results of the 56-day experiment also showed increases of 29 % to 48 %, 10 % to 23 %, 8 % to 22 %, and 33 % to 37 % over the control mixes, respectively.

3.1.2. Flexural strength testing for temperature effect

To evaluate the flexural tensile strength of the samples under the influence of temperature, the samples left to water cure for 28 days were taken from the curing tank and exposed to the temperature effect in an oven. After the samples were exposed to temperatures of 150 °C, 160 °C, and 180 °C, the values of the tests conducted with the samples taken from the curing tank (at a room temperature of 22 °C) were compared. The lowest flexural tensile strength values of the samples under the influence of 150 °C, 160 °C, and 180 °C temperatures were calculated as 2.45, 2.73, and 2.75 MPa, respectively (Figure 10). These values were obtained from the MC13 mixture, which is the control mixture with the highest binder dosage. At the maximum flexural tensile strengths, the tensile strengths were calculated as 4.45, 4.52, and 4.61 MPa for 150 °C, 160 °C, and 180 °C, respectively (Figure 10). These values were obtained in the MC4 mixture, which has the lowest binder dosage and the highest aggregate content. In addition, the change in the replacement ratio of the aggregate and GS in this mixture is 50 %. Compared to the control sample not exposed to heat, it was observed that the tensile strength at the minimum flexural tensile strength increased by 2 % to 15 % at 150 °C, 160 °C, and 180 °C. It was observed that the tensile strengths at the maximum flexural tensile strength at 150 °C, 160 °C and 180 °C increased by 3 % to 6 % compared to the control sample not exposed to heat (Figure 10).

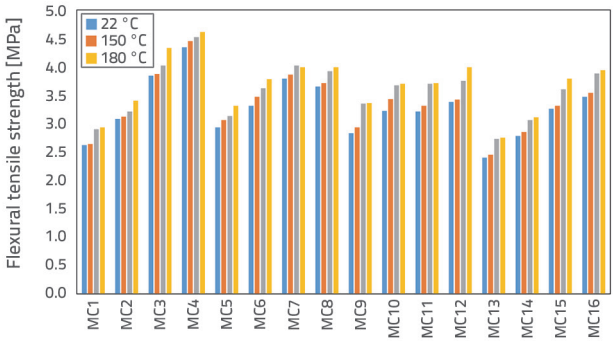

Figure 10. Temperature effect on flexural tensile strength

Mixture groups MC1–MC4, MC5–MC8, MC9–MC13, and MC14–MC16 were subjected to temperatures of 150 °C, 160 °C, and 180 °C, and the flexural tensile test results were then compared with the samples tested under laboratory conditions. Average increments of 1.4 %, 3.2 %, 3.5 %, and 2.0 % were calculated for the mixture groups MC1–MC4, MC5–MC8, MC9–MC13, and MC14-MC16, respectively, for samples extracted at 150 °C. At the end of 160 °C, average increases of 5.5 %, 7.3 %, 14.6 %, and 11.4 % were calculated for the same group ranking, respectively. Average increases of 10.1 %, 10.2 %, 16.8 %, and 14.1 % were respectively calculated after exposure to the final temperature step of 180 °C (Figure 10). The test results show that because the non-hydrated water in the mixture increases the hydration of the cement, the adhesion and compressive strength increase along with the temperature increase (25 °C to 180 °C) owing to the bond structure formed between the cement mortar and the GS and MA used. This shows that beyond 200 °C, this bond structure may decrease with an increase in temperature [36].

3.1.3. Flexural strength testing for freezing-thawing effect

A comparison of the flexural tensile strength results obtained at the end of the freeze-thaw test and the flexural tensile strength results obtained at 28 and 56 days for each sample set is shown in Figure 11. The MC13 and MC4 mixtures were calculated as having the lowest and highest flexural tensile strengths among the samples whose freeze-thaw tests were completed. The MC4 mixture has the lowest binder dosage but the highest microaggregate content. By contrast, the GS content in this mixture is 50 %. The MC13 mixture has the highest binder dosage but no GS content. At the end of the freeze-thaw cycles, the freeze-thaw strength loss varies between 3 % and 17 % compared to the 28-day samples. The lowest change calculated was for MC1, and the highest change occurred in MC16. However, MC1 was designed with the lowest binder dosage, whereas MC16 used the highest binder dosage. MC1 has no GS content, and MC16 has the highest GS substitution model the MC13–MC16 group (Figure 11).

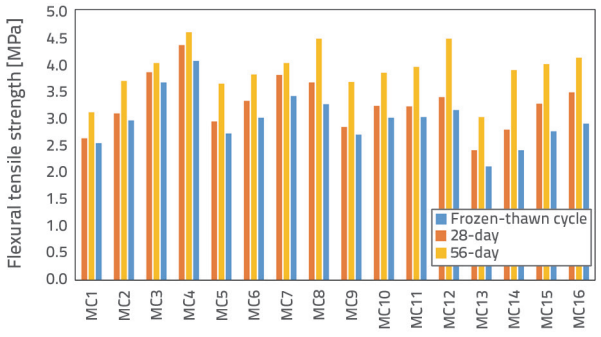

Figure 11. Flexural strength test of frozen-thaw cycles

In the samples with the highest GS content, there are surface cracks that can be observed on the outer surfaces of the samples because of the freeze-thaw cycles (Figure 12). By contrast, the freeze-thaw strength loss at the end of the freeze-thaw cycles varied between 9 % and 38 % compared to the 56-day samples. The lowest change was calculated in MC3, whereas the highest change was calculated in MC14. However, MC3 was designed with the lowest binder dosage, whereas MC14 used the highest binder dosage. The MC3 mix was designed to have a GS content of 27 %. The MC13 mixture, by contrast, has the highest binder content among the mixture groups produced with 12 % GS (Figure 12).

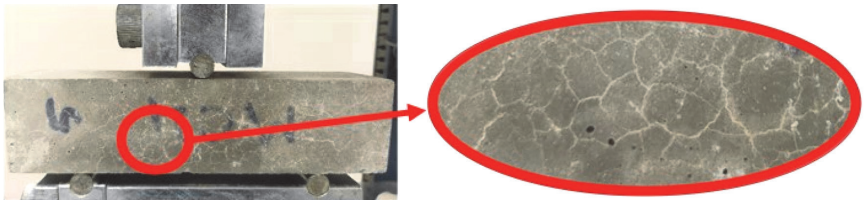

Figure 12. Samples after frozen-thaw cycles

3.2. Compressive strength

3.2.1. Compressive strength for standard age

After testing the flexural tensile strength values of the mixtures produced for 7-, 28-, and 56-day old specimens, the compressive strength test was applied to the parts obtained from the samples on the same day. The data obtained are presented in Figure 13. The minimum compressive strengths obtained for the 7-, 28- and 56-day samples were calculated as 42.57, 60.69, and 70.82 MPa. These compressive strengths were obtained from the samples produced from the MC8 mixture. In this mixture, the GS substitution rate used was 50 %. The maximum compressive strengths obtained for the 7-, 28-, and 56-day samples were calculated as 59.58, 68.07, 75.49, and 85.5 MPa (Figure 13). These strengths obtained were calculated in the MC13 mixture, and although it has the highest binder ratio in this mixture, there is no GS substitution. The changes in compressive strength were evaluated based on the control mixtures (MC1, MC5, MC9, and MC13) in the mixture groups. The changes in compressive strength obtained for 7 days of aging decreased between 4 % and 26 % with an increase in the GS substitution. However, these values varied between 1 % and 9 % for the 28-day age group, and between 3 % and 15 % for the 56-day age group. More importantly, an average reduction in compressive strength of 15 % was observed in mixtures with 50 % GS replacement (MC4, MC8, MC12, and MC16) (Figure 13).

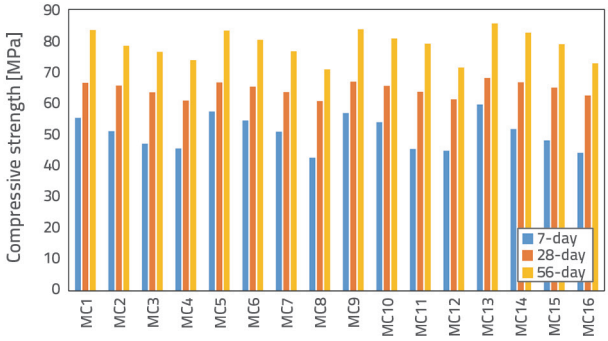

Figure 13. Compressive strength test results

3.2.2. Compressive strength for temperature effect

The samples obtained from the mixtures produced were evaluated in terms of the change in compressive strength after the effect of temperature at 150 °C, 160 °C, and 180 °C. The changes in compressive strength according to the 28-day old samples tested in the laboratory are presented in Figure 14. The lowest compressive strength of 62.22 MPa was obtained in MC4 at 150 °C. The lowest compressive strengths at 160 °C and 180 °C were observed in the MC12 mixture. As a common feature of the MC4 and MC12 mixtures, they have the highest GS content. The highest compressive strengths were obtained in the MC13 mixture samples tested after the effects of 150 °C, 160 °C, and 180 °C temperatures. These strengths were calculated as 72.34, 85.01 and 81.46 MPa, respectively (Figure 14). The samples that were dried in the laboratory environment were accepted as control samples within each group. These samples were evaluated in comparisons with the temperature effect. In this context, an increase in the samples of 1 % to 11 %, 2 % to 25 %, and 1 % to 20 % was observed at 150 °C, 160 °C, and 180 °C, respectively. As the GS content increased at 160 °C and 180 °C, the observed increases in compressive strength decreased from 20 % to 25 % to 2 % to 6 % (Figure 14). This might be due to the reaction of the $Ca(OH)_2$ compound, which can be formed from $CaCO_3$ in limestone sand, with SiO_2 in pozzolans (in GS and the addition of silica fume). As a result, the formation of calcium silicate hydrates, a by-product of the hydration reaction, is expected. As a result of these chemical reactions, the amount of $Ca(OH)_2$ may decrease and the available C-S-H increases [37–39]. It is thought that improving this situation with the effect of temperature may increase the performance of the MC within certain temperature ranges.

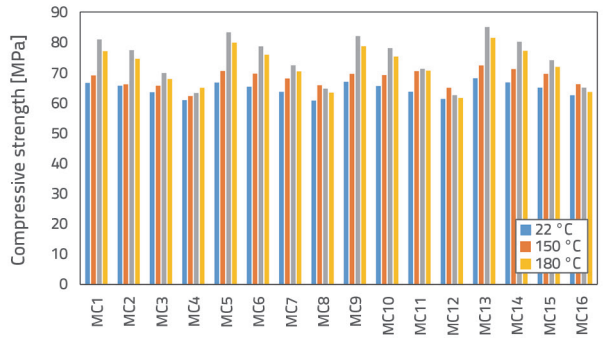

Figure 14. Temperature effect on compressive strength

3.2.3. Compressive strength for freezing-thawing effect

Prism-shaped samples obtained from the produced mixtures were subjected to the flexural tensile test described in the previous section after the freeze-thaw cycle, and compressive strength tests were then conducted on the broken prisms obtained. The compressive strength results are given in Figure 15, along with the 28- and 56-day results.

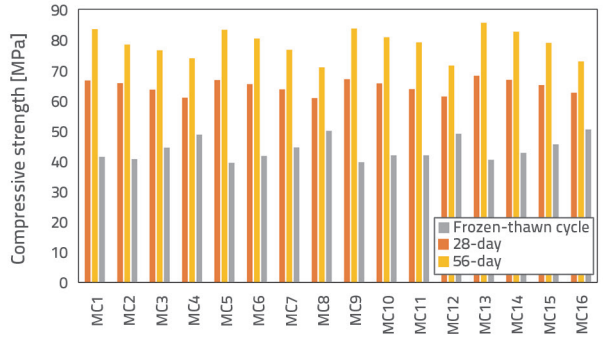

Figure15. Compressive strength test of frozen-thaw cycles

The compressive strength results obtained after the freeze-thaw cycle showed 19 % to 41 % losses in compressive strength compared to the samples tested at 28 days. By contrast, when the same evaluation was made according to the results of the 56-day samples, a loss of compressive strength of between 31 % to 53 % was calculated. In addition, the change in compressive strength of the samples produced from the mixtures containing 50 % GS (MC4, MC8, MC12, and MC16) was calculated respectively as 20 %–34 %, 18 % to 30 %, 20 % to 31 %, and 19 % to 31 % lower than the other mixtures among the group. These changes were calculated as having the lowest compressive strength loss owing to the freezing and thawing in their groups. Test images of the samples after a fracture are shown in Figure 16.

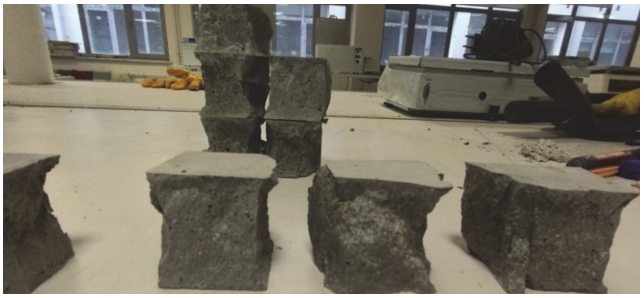

Figure 16. Compressive strength test samples of frozen-thaw cycles

3.3. Durability test results

3.3.1. Sorptivity

In the capillary water absorption test, the development of water movement from the concrete surface to the interior of the capillary systems formed by micro-sized voids was measured. This test is an important factor indirectly showing the permeability of concrete, that is, its durability. The absorbency graphs for mixture groups MC1–MC4, MC5–MC8, MC9–MC12, and MC13–MC16 are shown in Figure 17. Here, the S and I_0 values are calculated on the graphs obtained. The results of the obtained values are given in Figure 18. Regression coefficients were calculated as between 0.953 and 0.982. The lowest and highest sorption coefficients for the early age (S) were calculated as 0.013 and 0.046 (mm/min 0.5), respectively. In addition, the other calculated parameter, the first sorption (I_0), was calculated as having lowest and highest values of 0.081 and 0.292 (mm), respectively (Figure 18). The mixtures with the lowest and

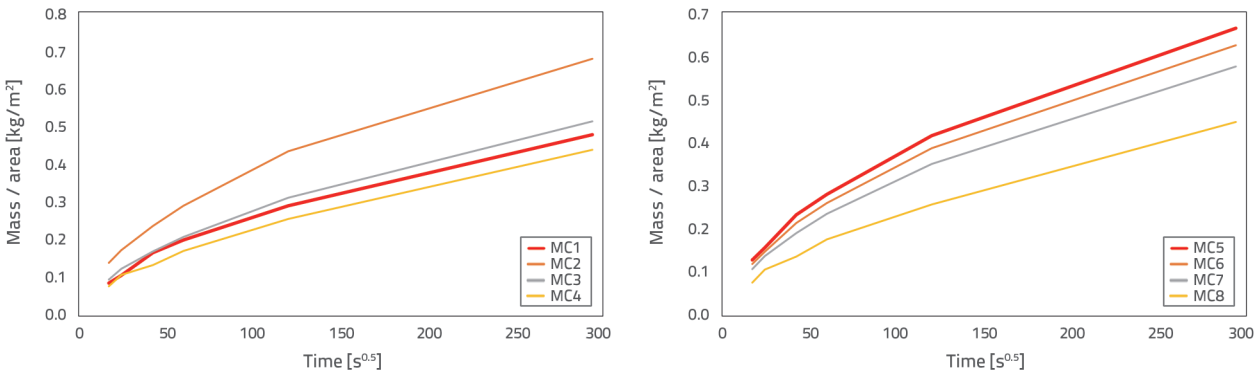

Figure 17. Sorptivity test results, 1st part of the figure

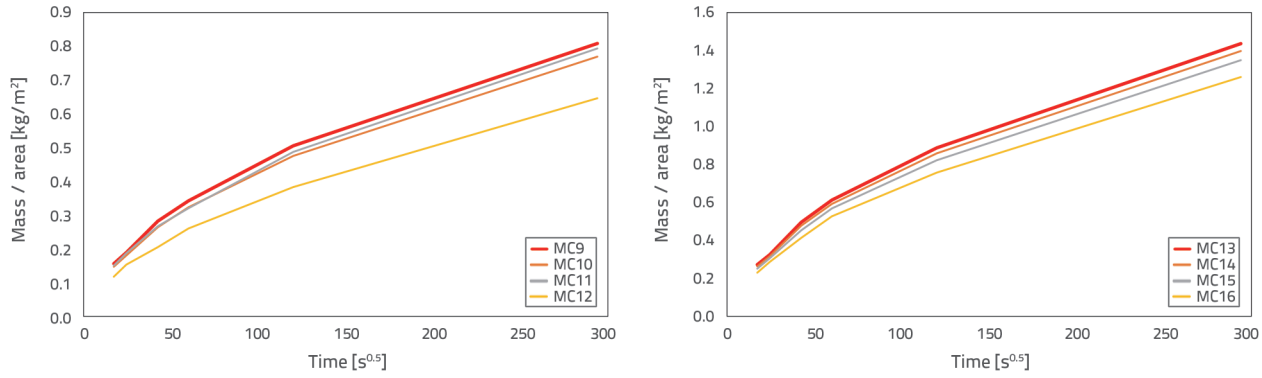

Figure 17. Sorptivity test results, 2nd part of the figure

highest values are MC4 and MC16, respectively. Both mixtures had the highest GS ratio (50 % substitution), whereas the latter had the highest binder dosage among the mixture groups.

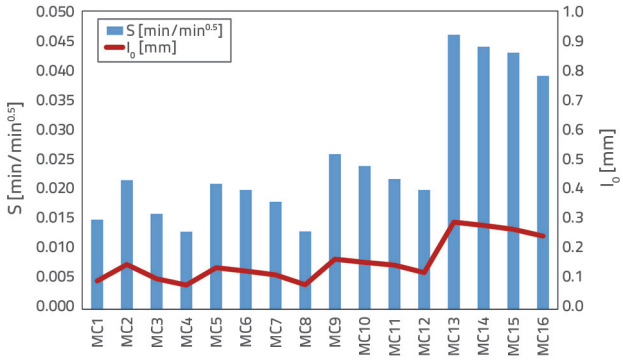

Figure 18. Sorptivity test results (S and I_0)

3.3.2. Porosity and specific gravity

The porosity values were calculated by dividing the difference between the saturated surface under a dry state and the oven dried state of the samples and their weight in water. These values were calculated by taking the average of three cube samples for each mixture within the scope of the present study. The results obtained were compared with the flexural tensile strengths of the 28-day samples and are given in Figure 19a. When the results were examined, the highest tensile strength was found to be 4.34 MPa for the 28-day samples, with a porosity value of 12.5 %. It was also demonstrated that the lowest flexural tensile strength corresponds to the highest porosity values among the groups of mixtures, and the lowest tensile strengths correspond to the lowest porosity values (Figure 19a).

The graph in Figure 19b examines the relationship between the compressive strengths and the changes in porosity. The graph shows that, among the results in the mixture groups, a decreasing porosity occurs in parallel with the decrease in compressive strength. The MC13 mixture, which has the highest compressive strength of 68.07 MPa, has a porosity of 20.7 %; however, this porosity corresponds to the lowest flexural tensile strength (Figure 19a, b).

In addition to the porosity test, bulk density calculations were also conducted on the samples produced within the scope of the present study. The resulting bulk density values varied between 2.2 and 2.41. In Figure 19a, which is a graph in which the flexural tensile strength and the bulk density are given together, the MC13 mixture shows the lowest flexural tensile strength, and the mass density converges at 2.4. In the MC4 mixture, where the highest flexural tensile strength is calculated, the mass density approaches 2.2 (Figure 19a). In addition, whereas the mass density converges to 2.4 in MC13, the mixture with the highest compressive strength,

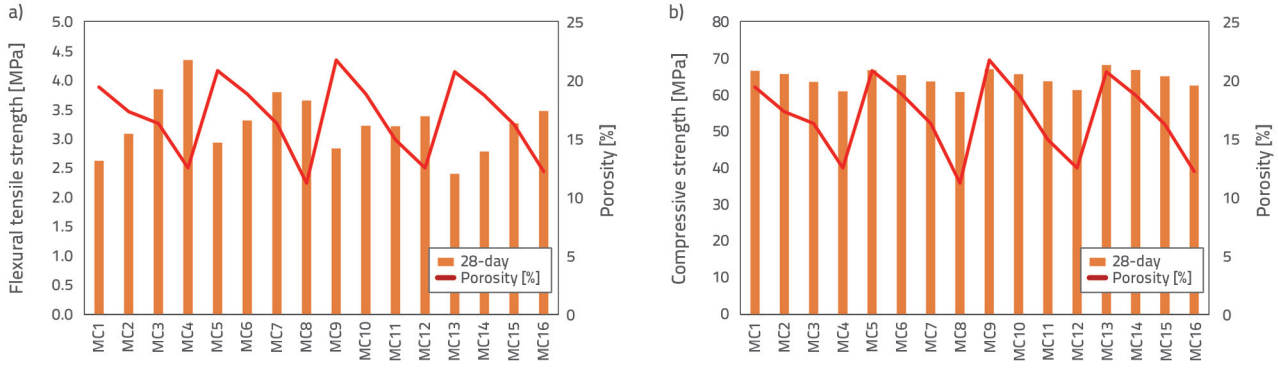

Figure 19. Porosity versus: a) flexural and b) compressive strengths

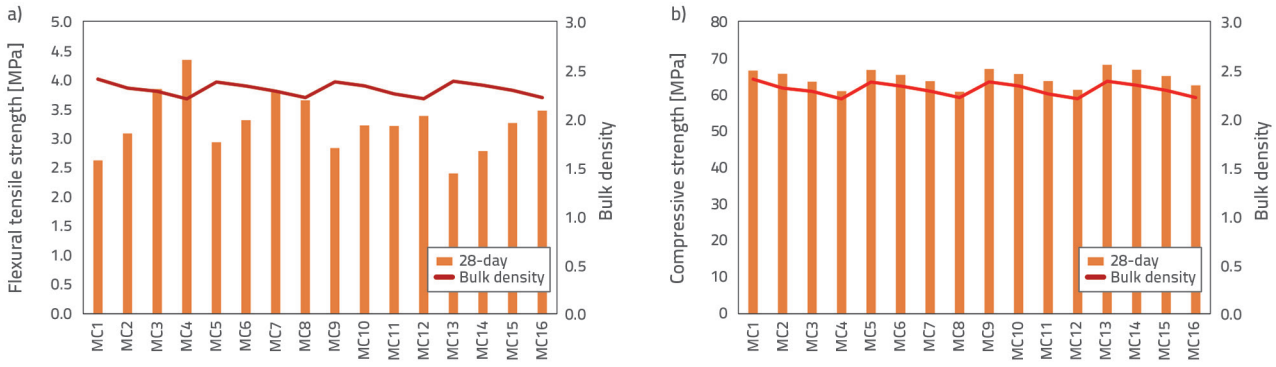

Figure 20. Bulk density versus: a) flexural and b) compressive strengths

it converges to 2.2 in the MC8 mixture, which has the lowest compressive strength (Figure 19b). The bulk density values decrease in parallel with the decreasing compressive strength among the mixture groups.

4. Conclusion

In this experimental study on the use of GS instead of MA in micro-concrete, the changes in flexural tensile and compressive strengths in terms of age, temperature, and freeze-thaw effect were examined and the following results were reached.

- Although having the same w/b ratio under a high binder dosage, it was observed that the GS substitute is effective in the bending tensile strengths at almost all ages. Moreover, considering the effect of increasing binder dosage, a slight decrease occurs in comparison to samples with a low binder dosage.
- GS substitution improves the flexural tensile strength as the substitution rate increases in mixtures within groups having the same binder dosage.
- Under the influence of applied temperatures of 150 °C, 160 °C, and 180 °C, significant increases in flexural tensile strength were observed, particularly at 160 °C and 180 °C.
- After 100 freeze-thaw cycles, the flexural tensile strengths of the samples exposed to this effect were calculated to decrease by 10 % on average compared to the 28-day samples. In addition, the flexural tensile strength decreased by an average of 25 % compared to the 56-day old samples.
- Despite a decrease in the compressive strength within the group in mixtures with a high binder dosage and GS substitution, significant increases were observed in the compressive strength between the groups.
- Although an increase in the compressive strength was shown under the influence of applied temperatures of 150 °C, 160 °C, and 180 °C, particularly at 150 °C and 160 °C, negative effects on the compressive strength occurred at 180 °C. This change occurred after reaching 160 °C when applying GS at 27 % and above, particularly in mixtures with a high binder dosage.
- When the compressive strengths obtained from the 28- and 56-day old samples are considered, the 100 freeze-thaw cycles resulted in average compressive strength losses of 32 % and 42 %, respectively. The greatest changes occurred in the control mixtures. GS substitution showed a positive effect and reduced the rate of decrease in strength.
- The use of GS caused a decrease in the porosity and bulk density while reducing the absorbency.
- According to the test results, mixtures containing MA and GS can be used in the placement of reinforcement anchors in areas requiring strengthening, in floor surface coatings in light and medium industrial structures, and in surface repair processes.

REFERENCES

[1] Long, G., Wang, X., Xie, Y.: Very-high-performance concrete with ultrafine powders, Cement and Concrete Research, 32 (2002), pp. 601-605.

[2] Felekoclu, B.: Effects of PSD and surface morphology of micro-aggregates on admixture requirement and mechanical performance of micro-concrete, Cement and Concrete Composites, 29 (2007), pp. 481-489.

[3] Mittal, M., Basu, S., Sofi, A.: Effect of Sika viscocrete on properties of concrete, International Journal of Civil Engineering (IJCE), 2 (2013), pp. 61-66.

[4] Karpuz, O., Akpinar, M.V., Aydin, M.M.: Effects of fine aggregate abrasion resistance and its fineness module on wear resistance of Portland cement concrete pavements, Revista de La Construccion, 16 (2017), pp. 126-132.

[5] Cemalgil, S., Etli, S., Onat, O.: Mechanical and Physical Properties of Self-Compacting Concrete Produced with Glass Powder, in: Int. Conf. Innov. Eng. Appl., Sivas, Turkey, 2018: pp. 371-376.

[6] Gesoglu, M., Güneyisi, E., Hansu, O., Etli, S., Alhassan, M.: Mechanical and fracture characteristics of self-compacting concretes containing different percentage of plastic waste powder, Construction and Building Materials, 140 (2017), pp. 562-569.

[7] Aïtcin, P.C.: Developments in the application of high-performance concretes, Construction and Building Materials, 9 (1995), pp. 13-17.

[8] Öz, H.Ö.: Fresh, Mechanical and Durability Properties of Self-Compacting Mortars Incorporating Waste Glass Powder and Blast Furnace Slag, Kahramanmaraş Sütçü İmam Üniversitesi Mühendislik Bilimleri Dergisi, 20 (2017), pp. 9-22.

[9] Zidol, A., Tognonvi, M.T., Tagnit-Hamou, A.: Effect of Glass Powder on Concrete Sustainability, New Journal of Glass and Ceramics, 07 (2017), pp. 34-47.

[10] Idır, R., Cyr, M., Tagnit-Hamou, A.: Use of waste glass in cement-based materials, Environnement, Ingénierie & Développement, N°57-Jan (2010).

[11] Shayan, A., Xu, A.: Performance of glass powder as a pozzolanic material in concrete: A field trial on concrete slabs, Cement and Concrete Research, 36 (2006), pp. 457-468.

[12] Schwarz, N., Cam, H., Neithalath, N.: Influence of a fine glass powder on the durability characteristics of concrete and its comparison to fly ash, Cement and Concrete Composites, 30 (2008), pp. 486-496.

[13] Aliabdo A.A., Elmoaty A.M., Aboshama A.Y.: Utilization of waste glass powder in the production of cement and concrete, Construction and Building Materials, 124 (2016),.

[14] Grdić, D., Ristić, N., Topličić-Ćurčić, G., Đorđević, D., Krstić, N.: Effects of addition of finely ground CRT glass on the properties of cement paste and mortar, Gradjevinar, 72 (2020), pp. 1-10.

[15] Artigas, V.F., Positieri, M.J., Quintana, M.V., Oshiro, Á., Cortez, F.R.: Self-compacting mortars with mineral additions: perlite and lime-stone filler, Revista de La Construccion, 20 (2021), pp. 479-490.

[16] Papadakis, V., Tsimas, S.: Supplementary cementing materials in concrete Part I efficiency and design, Cement and Concrete Research, 32 (2002), pp. 1525-1532.

[17] Matos, A.M., Sousa-Coutinho, J.: Durability of mortar using waste glass powder as cement replacement, Construction and Building Materials, 36 (2012), pp. 205-215.

[18] Saribiyik, A., Gurbuz, G.: Effects of glass fiber reinforced polymer pipe waste powder usage on concrete properties, Revista de La Construccion, 20 (2021), pp. 463-478.

[19] Gupta, N., Gupta, A.: Condition assessment of the structural elements of a reinforced concrete structure using non-destructive techniques, IOP Conference Series: Materials Science and Engineering, 1116 (2021), pp. 012164.

[20] Garg, S., Bajpai, K.K., Misra, S.: Rectification of a large vertical wall surface for flatness, Canadian Journal of Civil Engineering, 48 (2021), pp. 584-593.

[21] Felekoğlu, B.: High Performance Micro Concrete Design, (2009),.

[22] Felekoğlu, B.: Rheological behaviour of self-compacting micro-concrete, Sadhana - Academy Proceedings in Engineering Sciences, 39 (2014), pp. 1471-1495.

[23] ASTM C305/C305-20: Standard Practice for Mechanical Mixing of Hydraulic Cement Pastes and Mortars of Plastic Consistency, ASTM International, 04 (2009), pp. 3.

[24] Schwartzentruber, L.D.A., Le Roy, R., Cordin, J.: Rheological behaviour of fresh cement pastes formulated from a Self Compacting Concrete (SCC), Cement and Concrete Research, 36 (2006), pp. 1203-1213.

[25] ASTM C348-02: ASTM C348-02 Standard test method for flexural strength of hydraulic cement mortars, (2002), pp. 7.

[26] ASTM C349-08: Standard test method for compressive strength of hydraulic-cement mortars (using portions of prisms broken in flexure), ASTM Lnternational, (2008), pp. 1-4.

[27] ASTM: Standard Test Method for Resistance of Concrete to Rapid Freezing and Thawing, ASTM International, West Conshohocken, PA, 03 (2003), pp. 2-7.

[28] Leung, H.Y., Kim, J., Nadeem, A., Jaganathan, J., Anwar, M.P.: Sorptivity of self-compacting concrete containing fly ash and silica fume, Construction and Building Materials, 113 (2016), pp. 369-375.

[29] Hall, C.: Water sorptivity of mortars and concretes: A review, Magazine of Concrete Research, 41 (1989), pp. 51-61.

[30] ASTM C1585-13: Standard Test Method for Measurement of Rate of Absorption of Water by Hydraulic Cement Concretes, ASTM International, 41 (2013), pp. 1-6.

[31] Bentz, D.P., Ferraris, C.F., Wingpigler, J.: Service Life Prediction for Concrete Pavements and Bridge Decks Exposed to Sulfate Attack and Freeze-Thaw Deterioration, Volume II- Technical Basis for CONCLIFE- Sorptivity Testing and Computer Models, (2001),.

[32] Cemalgil, S., Onat, O., Tanaydın, M.K., Etli, S.: Effect of waste textile dye adsorbed almond shell on self compacting mortar, Construction and Building Materials, 300 (2021),.

[33] Torres, M.L., García-Ruiz, P.A.: Lightweight pozzolanic materials used in mortars: Evaluation of their influence on density, mechanical strength and water absorption, Cement and Concrete Composites, 31 (2009), pp. 114-119.

[34] ASTM C642-97: Standard Test Method for Density, Absorption, and Voids in Hardened Concrete, ASTM, (1997),.

[35] Galle, C.: Effect of drying on cement-based materials pore structure as identified by mercury intrusion porosimetry A comparative study between oven- , vacuum- , and freeze-drying, Cement and Concrete Research, 31 (2001), pp. 1467-1477.

[36] Ahmed, T.U., Shafiuddin Miah, Akhtar Hossain, Bari, N., Sazzad, M.: Effect of elevated temperature on the strength of cement mortar with the inclusion of fly ash, 29th Conference on OUR WORLD IN CONCRETE & STRUCTURES, (2004), pp. 135-141.

[37] Rostásy, F.S., Weiß, R., Wiedemann, G.: Changes of pore structure of cement mortars due to temperature, Cement and Concrete Research, 10 (1980), pp. 157-164.

[38] Lin, W.M., Lin, T.D., Powers-Couche, L.J.: Microstructures of fire-damaged concrete, ACI Materials Journal, 93 (1996), pp. 199-205.

[39] Khurram, N., Khan, K., Saleem, M.U., Amin, M.N., Akmal, U.: Effect of Elevated Temperatures on Mortar with Naturally Occurring Volcanic Ash and Its Blend with Electric Arc Furnace Slag, Advances in Materials Science and Engineering, 2018 (2018), pp. 1-11.